Mechanistic investigations towards a successful PET with Breslow-Intermediates

Jenny Phan [a] and Julia Rehbein*[a†]

Even under non-oxidativ thermal NHC-catalysis conditions Breslow-intermediates can undergo oxidations that feature NHC-stabilized radicals as transients. But how to harness these for specific synthetic purposes? Here, recent mechanistic studies are summarized to identify the prerequisites to achieve successful and universally applicable dual NHC-photoredox catalysis that enables the reagent-independent formation of NHC-stabilized ketyl radicals.

NHC-catalysis is a long established form of asymmetric organocatalysis[1] that allows for the umpolung of the inherent electrophilic character of carbonyls.[2] Rather late in regard to the methodological development and mechanistic postulates and associated studies[3,4] the idea evolved that single electron transfer (SET) or proton-coupled electron transfer (PCET) may play a role in the pathways involving the key enaminol structure **EA** (Scheme 1).[5,6,7] Detailed studies regarding the origin of EPR-observable open-shell structures (**R**) and their potential role within the NHC-catalytic cycle let to the conclusion that most likely the Breslow intermediate is the direct precursor of such NHC-stabilized ketyl type radicals (**OH-EA-R**, **EA-dep-R**). Structures like **EA-dep-R** have been proposed in the oxidative NHC-catalysis, but only as an intermediate to the full-two-electron oxidation to feature acyl azolium species.[8] Rather lately Studer has shown a dual catalysis using photoredox catalysts to oxidise acyl azolium intermediates.[9] Our interest evolves around the differentiation of the reactivities of the various possible radical structures and their selective formation, i.e. to derive a universal reactivity map under given reaction conditions. As depicted in Scheme 1, one can classify these radicals **R** according to their charge (neutral: **EA-dep-R**, **OH-PA-R**; cationic: **OH-EA-R**, anionic: **PA-dep-R**) and their ability to accept or donate a hydrogen atom. Hence, quite different chemoselectivities and pathways are expected. Since standard Breslow intermediates (**EA**) and primary adducts (**PA**) are rather fleeting in nature, we decided to make use of the stable *O*-methylated derivates for our mechanistic studies.

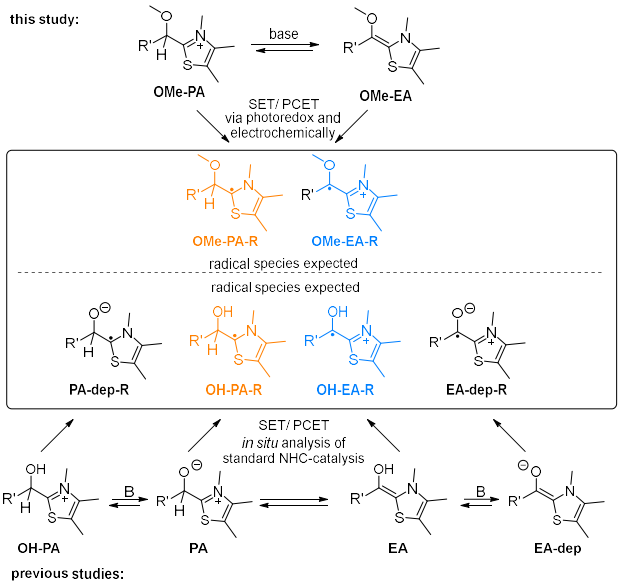

Scheme 1. The key structure of standard NHC-catalysis cycles (bottom part) in the activation of simple aldehydes. The radicals **EA-dep-R** and **OH-EA-R** were previously characterized and analyzed regarding their reactivity and their most likely pathway of formation. Highlighted are the similarities between the here studied O-methylated radical species **OMe-PA-R** and **OMe-EA-R** formed via photoredox catalysis and electrochemistry.

This approach has the advantages that we have defined starting points for the interaction with the photocatalysts and for electrochemical conversions, it reduces the number of possible acid-base and other pre-equilibria and can test for the broad range of substrate electronics. The following results hence mimic the situation where the Breslow-intermediate is in its neutral state (**EA**) and the primary adduct in its cationic form. These two structures are the ones that are most likely to occur under the widely used protic conditions in standard NHC-catalysis and have also been identified by NMR spectroscopy.[3,4] The synthesis of **OMe-PA** and **OMe-EA** for R' = Ph was accomplished as previously described. [10, 11, 12]

Following general questions are addressed: Which conditions are needed to have an efficient photoelectron transfer from the excited state photocatalyst (PC*)? Will the photoredox step involving the PC* take place with the enaminol **OMe-EA** selectively or are site-reactions expected with the primary adduct **OMe-PA**? In this regard, how are the **OMe-EA** and the **OMe-PA** linked via redox-steps (SET vs. PCET). The answers were sought by a combination of photophysical experiments, like quenching studies and spectro-electro chemistry.

Based on previously published CV-data the choice of photoredox catlaysts was made.[5] $[Ru(bpy)_3]^{2+}$ and Eosin Y both have enough redox-potential to access the according SET-derived radicals from primary adduct **OMe-PA** and Breslow-intermediate **OMe-EA**. To avoid complications due to the pH-

dependence of the structure of Eosin Y, the disodium salt was used (Na_2Eosin Y).

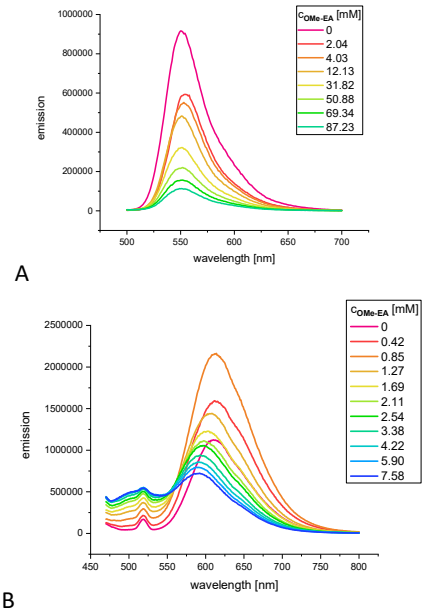

Figure 1. A. Excitation of Na_2Eosin Y with 480 nm, emission in the 500-700 nm range that was quenched by **OMe-EA** (slit width 1 nm). B. Same quenching experiment with $[Ru(bpy)_3]Cl_2$ as fluorophore. Here first an increase than a decline of the fluorescence is observed accompanied by a shift in the emission wavelength.

The quenching of the two (Table 1, Figure 1) photoredox-catalysts with **OMe-PA** and **OMe-EA** with and without sacrificial oxidant or reductant showed that only the Breslow-intermediate **OMe-EA** was able to quench the PC*. That the quenching process furnishes a photo electron transfer (PET) is confirmed by the EPR-spectra taken during irradiation of the same reaction solutions (Figure 3, additional information see ESI). With **OMe-EA** a radical species was formed whereas in case of **OMe-PA** the reaction solution remained EPR-silent. These results suggest that also under standard catalysis conditions (in protic polar media) with transients **OH-PA** and **EA** being present the PET will selectively take place with **EA**. In regard to the choice of photocatalyst the quenching constants suggest that the Na_2Eosin Y is a good lead-structure, with a quenching rate constant being 5.7 x 10^4 times higher than with $[Ru(bpy)_3]Cl_2$ (Table 1).

Table 1. Overview of the quenching experiments with **OMe-EA** using two different PCs and reductive (DIPEA) and oxidative additives (*m*-dinitrobenzene, *m*-DNB).

		$[Ru(bpy)_3]Cl_2$			Na_2Eosin Y		
#	add.	K_{sv}[a]	k_q [b]	EPR	K_{sv}[a]	k_q [b]	EPR
1	DIPEA	1.08	0.03	X	0.699	5.78	X
2	none	1.08	4.51	X	74.3	614	X
3	*m*-DNB	55.3	1.58	X	78.5	649	X

[a][L·mol^{-1}]. [b] x 10^8 [L·(mol·s)$^{-1}$]

The *in situ* EPR-spectra taken under irradiation of the reaction solution at 530 nm (Na_2Eosin Y) and 455 nm ($[Ru(bpy)_3]Cl_2$) were used to decide on the possible requirement of sacrificial electron donors or acceptors. As a read-out for the efficiency of the SET process the intensity (double integration of the observed signal) of the EPR-spectra were used to determine when the formation of the ketyl-type radical species is highest (Table 2). In line with the highest quenching rate of the Breslow intermediate **OMe-EA** without any additive and Na_2Eosin Y yielded the highest spin concentrations.

Table 2. Observed changes in the EPR-intensities with the two different PCs and different additives.

#	PC	additive	EPR intensity [a,b]	relative EPR intensity
1	Na_2Eosin Y	none	792	7.0
2	Na_2Eosin Y	Pyridine	521	4.6
3	Na_2Eosin Y	DIPEA	218	1.9
4	Na_2Eosin Y	TEA	175	1.5
5	Na_2Eosin Y	$K_2S_2O_8$	343	3.0
6	$[Ru(bpy)_3]Cl_2$	Pyridine	430	3.8
7	$[Ru(bpy)_3]Cl_2$	$K_2S_2O_8$	113	1.0 (ref.)

[a] after 10 min of irradiation. [b] based on integrated area (double integration of observed signal)

In presence of additives not only the quenching rates of PC* are partially lowered (amines) but also the radical concentrations in comparison to the reaction solutions without any additives. The latter observation can either be explained by three different scenarios: First, the competition between additive and **OMe-PA** in the quenching of the PC*. Second, by an onwards reaction of the formed **OMe-PA-R** with the additive to a closed shell species. Third, by an effective pre-complexation of PC or **OMe-EA** prior to irradiation which is suspended or triggered by the presence of an additive. Based on the independent quenching rates measured for the two PCs by the different additives in comparison to **OMe-EA** (Table 3) the first hypothesis may be applicable for the oxidizing, but not for the reducing additives. In case of the reducible additives (*m*-DNB, $K_2S_2O_8$) the quenching rates are very similar to the ones of **OMe-EA** and hence the observation of unchanged quenching constants but lower amounts of **OMe-EA-R** may be explained by a competition for PC* (Table 3, Entries 2, 3, 8, 9).

Table 1. Comparison of the quenching rates k_q of the additives and **OMe-PA** in degassed THF.

#	PC	Q	K_{SV}[a]	k_q [b]	$k_{q,rel}$
1		DIPEA	8	6.68	1
2	Na_2Eosin-Y	mDNB	600	496	74
3		**OMe-EA**	773	639	96
7		DIPEA	11	0.03	1
8	$Ru(bipy)_3Cl_2$	mDNB	695	20	667
9		**OMe-EA**	700	20	667

[a] x 10^{-4} [L/mol]. [a] x 10^8 [L/mol/s]

If amines are used the situation is somewhat different. **OMe-EA** is 96 (Na_2Eosin Y) to 667 ($[Ru(bpy)_3]Cl_2$) times faster than the amine in quenching the PC*. Still the quenching rate of PC* in

the reaction solution is diminished for both PCs as well as the concentration of **OMe-EA-R** (Table 2).

The above mentioned hypothesis of assembly formations of the three components in different permutations like PC•**OMe-EA**, PC•PC or **OMe-EA**•amine was pursued first. Although Brønsted acid-base interactions with **OMe-PA** and the amine prior to irradiation seem unlikely, UV-vis spectra of **OMe-EA** recorded as a function of c_{DIPEA} and by the quenching studies of the **OMe-EA** fluorescence (Figure 2) suggest an association of the two molecular structures already in the electronic ground state.

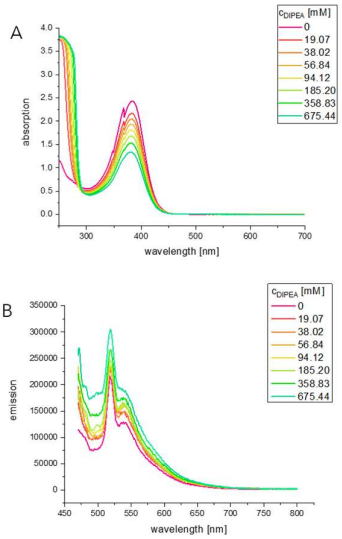

Figure 2. A: UV-vis absorption spectra of **OMe-EA** during the titration with DIPEA. The absorption maximum decreases continuously with the base concentration indicating a complex formation in the electronic ground state. B: Fluorescence quenching of **OMe-EA** with DIPEA; irradiation at 450 nm (slit-width: 6 nm), emission: 470–800 nm (slid width: 6 nm)

As both, UV-vis absorption and fluorescence are continuously decreased and enhanced respectively with rising base concentrations an assembly formation already in the electronic ground state between these two molecular species is likely. This type of assembly is deemed to be undesired as it apparently leads to a less efficient quenching of PC*. That a similar assembly between PC and **OMe-EA** prior to the SET step especially between $[Ru(bpy)_3]Cl_2$ and **OMe-EA** is a likely option can be derived from the quenching experiments shown above (Figure 1B). The shift of the wavelength and initial increase of the fluorescence upon continuous addition of **OMe-EA** indicate a molecular association step of both structures. Such an assembly might allow for a very efficient PET. Therefore, the efficiency of this interaction between PC and **OMe-EA** was studied further by determining the possibility of a dark redox-reaction between PC and **OMe-EA**, that would require and hence prove the pre-association of both structures independently of the Stern-Volmer quenching studies (Figure 3B-D). In case of both photocatalysts (PC) the radical concentration in presence of **OMe-EA** and pyridine or $K_2S_2O_8$ is significantly above zero even without light (Figure 3B-D).

Figure 3. EPR monitoring of the reaction solutions (**OMe-PA**, PC (5 mol%), 2 eq or no additive in degassed THF) during irradiation at t =10 min: A) with Na_2Eosin Y (λ_{irr} = 530 nm) and different amine bases (2 eq) ; B) comparison with $[Ru(bpy)_3]_2Cl_2$ and 2 eq pyridine (λ_{irr} = 455 nm) C) Na_2Eosin Y in presence of pyridine (2 eq) without irradiation. D) Comparison of dark background reaction in dependence of PC and **OMe-EA-R**. measurement conditions: mean field 337.784 mT, width: 8.305 mT, µwave power: 10 mW, t: 30 s, amplitude of modulation: 0.7 mT, reciever gain: 10 dB.

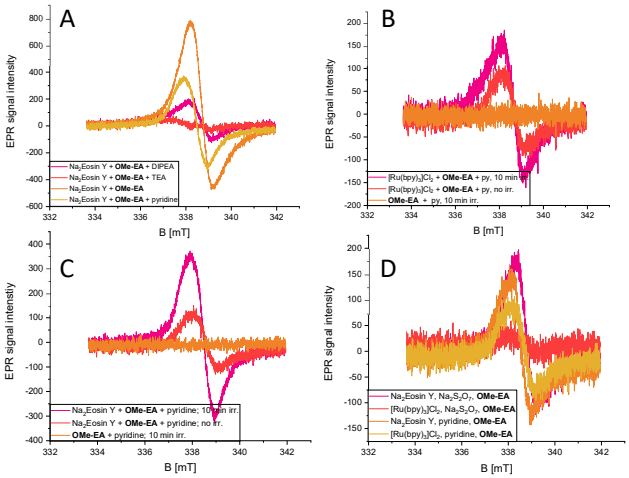

In case of the oxidative additives the oxidation of the **OMe-EA** can take place. If amines are used for a reductive quench of PC* this rational is not applicable. However, further control experiments by EPR spectroscopy could show that it is not the PC itself or its interaction with pyridine (see ESI) or an interaction between pyridine and **OMe-EA** that gave rise to the observed dark reaction. This leaves a thermally activated SET process within an assembly of **OMe-EA** and PC as the only rational.

With this assembly in place the hypothesis of the amine acting as a reactant for **OMe-EA-R** is not ruled out yet. Therefore, the

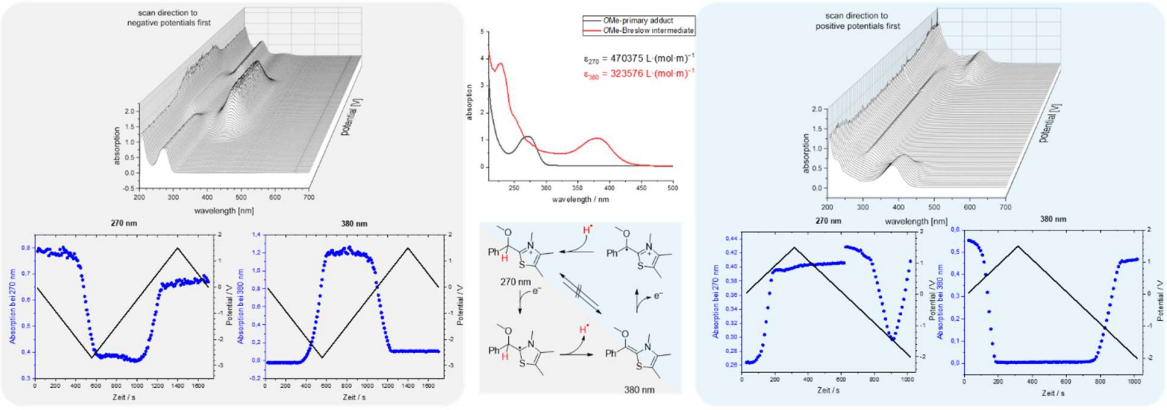

Figure 4. Summary of the spectro-electrochemical studies of **OMe-PA** (left) and **OMe-EA** (right) in THF using the UV-vis absorption as a read out to identify the resulting intermediates. Clearly there is a PCET interconnection under these electrochemical conditions between **OMe-PA** and **OMe-EA** that most likely is mimicked under photoredox-catalytic conditions in presence of HAT-donors/acceptors.

concentration of **OMe-EA-R** was measured by EPR in dependence on the amine structure. Since reactions with TEA and also DIPEA led to a stronger loss in radical concentration than pyridine (Figure 3A) a HAT pathway from amine to **OMe-EA-R** seems most likely. Consequences for an attempted dual catalysis approach would be to avoid amine bases that feature HAT reactivity, since these can apparently transform the **OMe-EA-R** derived from the PET process of the **OMe-EA** back into the photoredox inactive primary adduct **OMe-PA**. The direct HAT-relationship between the protected Breslow- and primary adduct was shown in an independent set of spectro-electrochemical experiments (Figure 4).

To elucidate further if the hypothesis of a direct transformation of **OMe-EA** to **OMe-PA** and vice versa via a PCET is possible spectro-electrochemical experiments were conducted. Hereby, the UV-vis spectra were record whilst driving the potential of the electrochemical cell until oxidation or reduction peak potentials of **OMe-PA** and **OMe-EA** were reached (Figure 4). The UV-vis spectra of **OMe-PA** and **OMe-EA** have characteristic absorption bands that allow for an unambiguous identification of these structures (Figure 4, center).

Starting with the **OMe-PA** the scan direction was first going towards negative potentials and then reversed. Opposite scan-directions were used to study the UV-vis spectra of the electrochemically derived intermediates of **OMe-EA**. This choice of scan directions resulted from the previously conducted cyclovoltammetry measurements (see ESI) and were corroborated by the observation that only then changes in the UV-vis spectra are observed (Figure 4, top).

The UV-spectra recorded in dependence of the potential indicate that the **OMe-PA** will become – after a SET reduction – a potent hydrogen atom donor, leading to the **OMe-EA** after a HAT step. In this electrochemical experiment the only HAT-acceptor is the solvent. But one can envision substrates that can be reduced via HAT under these electrochemical conditions. The inverted behavior is observed for the **OMe-EA**. After a SET oxidation the resulting **OMe-EA-R** will quickly capture a hydrogen atom to return to the closed shell **OMe-PA**.

Conclusions

In this study the interconversion via PCET between **OMe-PA** and **OMe-EA**, i.e. the stable derivatives of the primary adduct (cationic form) and the Breslow intermediate (neutral form) have been shown by spectro-electrochemistry. Under photoredox catalysis conditions only the enaminol **OMe-EA** was able to quench the excited state of the photocatalyst (PC), raising the expectation that the in a dual catalysis approach the PET will be selective for **EA**. The PET step produced an EPR signal that has been previously characterized to be the radical from a SET oxidation of **EA**. The reductive quench cycle hence is in operation. Combined quenching and EPR studies suggest, that amine additives that can undergo hydrogen atom transfer (HAT) are counterproductive as these return the **OMe-EA-R** into the unreactive **OMe-PA**. Also, experimental evidence has been found for a productive (SET reactive) ground state assembly between PC and **OMe-EA** as well as a counter-productive amine-**OMe-EA** complex. Based on these fundamental mechanistic insights synthetic applications like the dual NHC-photoredox catalysis targeting the Breslow intermediate as the reductant for the photocatalyst are currently worked on and will be published in due course.

Author Contributions

JP run the investigations, JR was responsible for the conceptualization and write-up of the original manuscript.

Conflicts of interest

There are no conflicts to declare.

Acknowledgments

JR thanks the DFG for the generous financial support by of the Emmy-Noether funding scheme, RE3630/1.

Notes and references

1 R. Kluger and K. Tittmann, *Chem. Rev.* 2008, **108**, 1797.
2 R. Breslow, *J. Am. Chem. Soc.* 1958, **80**, 3719.
3 M. J. White and F. J. Leeper, *J. Org. Chem.* 2001, **66**, 5124.
4 (a) M. Paul, M. Breugst, J.-M. Neudörfl, R. B. Sunoj and A. Berkessel, *J. Am. Chem. Soc.* 2016, **138**, 5044. (b) A. Berkessel, V. R. Yatham, S. Elfert and J. -M. Neudörfl, *Angew. Chem. Int. Ed.* 2013, **52**, 11158. (c) A. Berkessel, S. Elfert, V. R. Yatham, J. -M. Neudörfl and N. E. Schlörer 2012, **51**, 12370. (d) A. Berkessel, S. Elfert, K. Etzenbach-Effers and J. H. Teles, *Angew. Chem. Int. Ed.* 2010, **49**, 7120.
5 (a) J. Phan, S.-M. Ruser, K. Zeitler and J. Rehbein, *Eur. J. Org. Chem.* 2018, **2**-**3**, 557. (b) J. Rehbein, S.-M. Ruser and J. Phan, *Chem. Sci.* 2015, 6, 6013.
6 V. Regnier, E. A. Romero, F. Molton, R. Jazzar, G. Bertrand and D. Martin, *J. Am. Chem. Soc.* 2019, **141**, 2, 1109.
7 M.-H. Hsieh, G.-T. Huang and J.-S. K. Yu, *J. Org. Chem.* 2018, **83**, 15202.
8 J. Guin, S. De Sarkar, S. Grimme and A. Studer, *Angew. Chem. Int. Ed.* 2008, **47**, 8727.
9 Q.-Y. Meng, N. Dçben and A. Studer, *Angew. Chem. Int. Ed.* 2020, **59**, 19956.
10 V. Capriati, S. Florio, G. Ingrosso, C. Granito and L. Troisi, *Eur. J. Org. Chem.* 2002, 478.
11 G. Barletta, A. C. Chung, C. B. Rios, F. Jordan and J. M. Schlegel, *J. Am. Chem. Soc.* 1990, **112**, 8144.
12 B. Maji and H. Mayr, *Angew. Chem. Int. Ed.* 2012, **51**, 10408.